Clin Oral Invest (2011) 15:983–991
DOI 10.1007/s00784-010-0454-2

ORIGINAL ARTICLE

Healing of acute alveolar bone dehiscence following treatment with porous biphasic calcium phosphate in beagle dogs

Lanlei Wang · Han Shi · Yijia Chen · Jing Xue · Yangxi Chen · Yunmao Liao

Received: 21 May 2009 / Accepted: 26 July 2010 / Published online: 10 August 2010
© Springer-Verlag 2010

Abstract The purpose of the present study was to evaluate histologically in beagle dogs the healing in acute dehiscence type defects following treatment with open flap debridement (OFD) with or without porous biphasic calcium phosphate (PBCP). Alveolar bone dehiscence defects were surgically created bilaterally at the labial aspects of maxillary third incisors in 12 beagle dogs. After root conditioning with ethylenediaminetetraacetate, PBCP was filled in the defects and the contralaterals were cured with OFD. Two fluorochrome labelings were administered at the 7th and 11th weeks, respectively. Four dogs were killed at the 12, 16, and 24 weeks, respectively. Histological observations were processed through microcomputed tomographic imaging, fluorescence microscope, and light microscopy. The formation of new regenerated tissues was assessed histomorphometrically. The results revealed the healing after treatments with PBCP evidenced a new attachment apparatus and that with OFD supported periodontal repair. In PBCP groups, the amount of new bone varied from 1.15 to 3.86 mm (23–77.2% of the original defect size), while only 0.3 to 1.04 mm (6–20.8%) in OFD group. The amount of new cementum in PBCP varied from 1.18 to 4.16 mm (23.6–82.3%), while only 0.67 to 1.15 mm (13.4–23%) in OFD group. The amount of periodontal ligament in PBCP varied from 1.03 to 4.12 mm (20.6–82.4%), while only 0 to 0.93 mm (0–18.6%) in OFD group. There was significantly more regenerated tissue in PBCP groups compared to OFD procedures ($p<0.01$). The present results indicate that PBCP may enhance periodontal regeneration in acute-type labial dehiscence defects.

L. Wang · H. Shi · Y. Chen · J. Xue · Y. Chen (✉) · Y. Liao
State Key Laboratory of Oral Diseases, Sichuan University, Chengdu, People's Republic of China
e-mail: 406975817@163.com

Keywords Periodontal regeneration · Porous biphasic calcium phosphate · Porosity · Bone graft · Scaffold

Introduction

The complete and predictable restoration of the periodontium following trauma or infection remains a critical objective in periodontics. Periodontal regeneration is defined as the reconstruction of the damaged periodontium as evidenced histologically in the formation of cementum, a functionally oriented periodontal ligament (PDL), and alveolar bone. The interaction between the hard and soft tissues makes periodontal wound healing a complex process. It has been suggested that the epithelial cells at the early stage of the periodontal healing demonstrate the highest capacity of proliferation among periodontal tissues involved in wound healing, so they first repopulate the exposed root surface in defects and form a long junctional epithelium after periodontal surgery [1, 2]. To date, various treatment modalities such as implantation of bone graft materials, chemical root conditioning, guided tissue regeneration, growth factors, and combination of these approaches have been employed in clinical practice. However, the clinical results obtained with these methods vary widely and are often unpredictable [3–7].

In clinical practice, bone grafts are widely used in the treatment of periodontal osseous defects. But it is generally accepted nowadays that bone grafting materials alone function as defect fillers and induce periodontal regeneration unpredictably.

Currently used grafts for medical purpose include autografts, allografts, xenografts, and artificial grafts, etc. But limited availability of autografts and potential by infection of allografts produce an increasing demand on

artificial bone grafts. Among a variety of synthetic bone substitute materials, calcium phosphate bioceramics are promising due to similarity of their chemical composition to that of bone mineral. At first, hydroxyapatite (HA) itself was the focus of attention because of its bioactivity. However, it soon turned out that HA had some inherent drawbacks such as limited degradation. In order to intensify the biodegradation, biphasic composites of HA and biodegradable material, such as HA/β-tricalcium phosphate (β-TCP), have been studied as an alternative to HA ceramics [8]. In 1986, the material with the weight ratio of HA/β-TCP 20:80 was firstly implanted in periodontal osseous defects and was confirmed its efficacy [9]. This material was later described as BCP and subsequently developed with varying HA-to-β-TCP ratios.

During the last 20 years, BCP with a porous structure has been investigated extensively. Its macropores provided space for bone ingrowths, and its micropores allowed the transportation of body fluid, which led to angiogenesis and helped tissue regeneration. However, a material generally weakens as its porosity increases. The poor mechanical strength of PBCP ceramics often limits their use in the cases of important stresses in clinical practice. Most PBCP bioceramics are applied in filling the small bone defects or the bone defects with large contact with host bone [10–13].

With osteoconduction, biocompatibility, and osteointegrative properties, PBCP has already been proven its efficacy on bone regeneration in trauma and orthopedic surgery. More recently, several studies have reported that PBCP could induce ectopic bone formation after implantation in soft tissue sites of large animals such as dogs and sheep [14–18]. PBCP with appropriate 3D geometry may be favorable for the adsorption and accumulation of endogenous bone growth factors in circulation such as bone morphogenetic proteins and transforming growth factor-β1 [19, 20].

Currently, a great improvement has been made on the understanding of cellular and molecular events involved in the regeneration of periodontal tissues. Periodontal regeneration may be facilitated by allowing more time and space for only cells from bone tissues and PDL to repopulate the root surface in the defect. When PBCP is implanted into a periodontal osseous defect as a barrier and filler, its porous structure can provide protective spaces in the excavations or inside the pores. Although some preliminary data from in vitro studies suggest that PBCP may have a positive effect on periodontal ligament and bone cells, it is unknown at present to what extent this material may facilitate periodontal wound healing and regeneration.

In a previous study, we had confirmed the efficacy of PBCP on periodontal regeneration although the volume of periodontal regeneration was still far from being ideal [21]. The purpose of the present study is to evaluate the healing of surgically created alveolar bone dehiscences in beagle dogs following treatment with and without PBCP.

Materials and method

Biomaterial preparation

In our study, PBCP was supplied by the Material Lab of West China College of Stomatology Sichuan University (PBCP, 0801, Chengdu, China). The pore texture was regulated by porogen. Raw materials were diammonium hydrogen phosphate, calcium nitrate, and ammonia. The raw materials of given proportion were mixed by the end products of PBCP with 40HA/60β-TCP. After a complete reaction, the slurry was stirred mechanically at room temperature for 24 h and then centrifuged, filtered, and dried at 60°C for 8 h, and it was heated at the rate of 10°C/min up to 1,200°C, held at this temperature for 1 h, and then cooled in the furnace. Finally, PBCP samples were cut into cubes (Fig. 1a).

The 3D images from microcomputed tomography (μCT) imaging and analysis (μCT80, Scanco Medical AG, Bassersdorf, Switzerland)) exhibited that the porosity of the materials was 85% and the macropores were interconnected. The average macropore diameter is of 162 μm (range, 116–515 μm), and the mean wall thickness is of 66 μm (range, 36–144 μm; Fig. 1b, c). XRD photograph of PBCP showed that only HA and β-TCP phases were defected, so PBCP had no impurity (Fig. 1d). The photos of PBCP by SEM revealed that the macropores were uniform, and abundant micropores were distributed in the wall of macropores (Fig. 1e, f). The micropore size was about 2–10 μm (ranges from 100 nm to 10 μm).

Animals

Twelve 1.5-year-old male beagle dogs (body weight 9.5± 1.6 kg) were used in this study. The animals exhibited a fully erupted, healthy, permanent dentition. They were offered by the Experimental Animal Centre of Sichuan University (Chengdu, China). The study protocol was approved by the Animal Ethical Committee for Animal Research of Sichuan University (Chengdu, China). During the experiment, the dogs were fed with soft-food diet and water to minimize mechanical trauma to the flaps. The experimental started after an adaptation period of 1 week.

Four dogs were sacrificed by means of sodium pentobarbital overdose at 12, 16, and 24 weeks after implantation, respectively. The experimental teeth together with surrounding tissue were immediately dissected and fixed in 70% ethanol for 3 days. Scanned by micro-CT, the specimens were processed undecalcified for bone histological analysis.

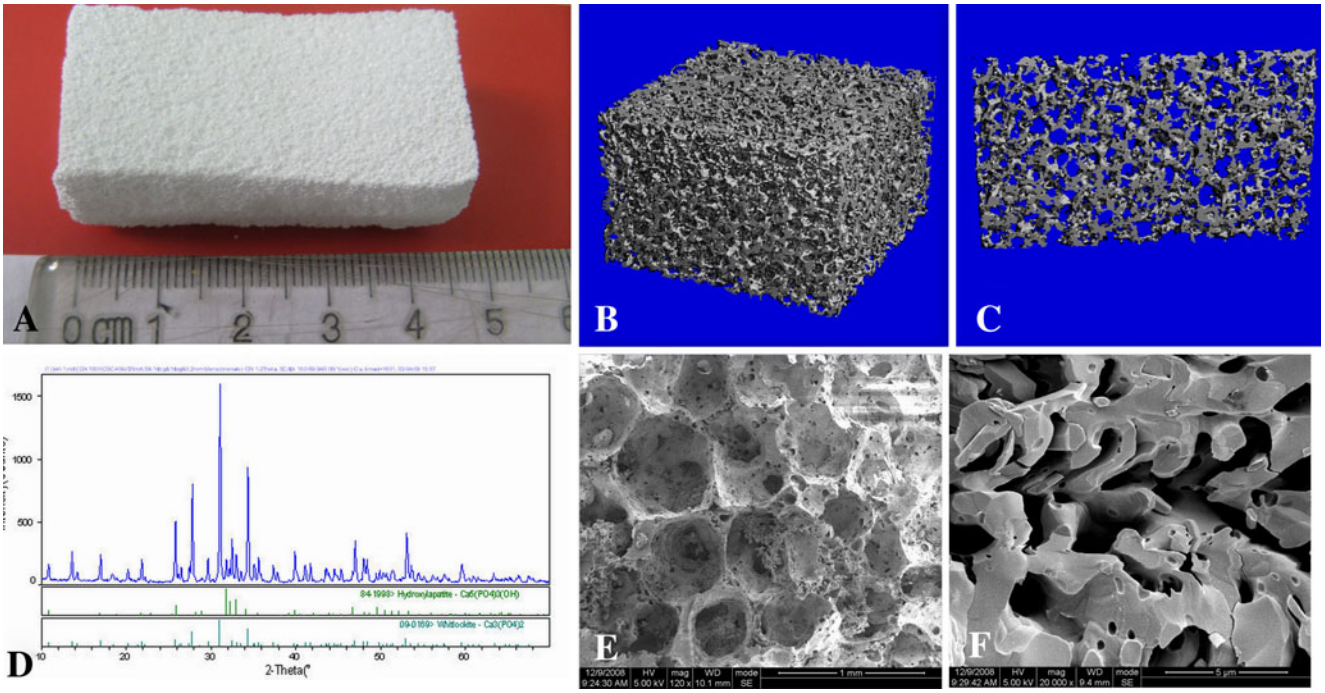

Fig. 1 Structural profile of PBCP. **a** The aspect of PBCP sample; **b** 3D reconstruction image of BCP by μCT; **c** reconstruction transect image of PBCP by μCT; **d** XRD photograph of PBCP showed that only HA and β-TCP phases were defected; **e** SEM micrographs of macropores in PBCP block (×120). *Bar scales*, 1 mm; **f** SEM micrographs of micropores in the wall of macropores, magnified view of **b** (×20,000). *Bar scales*, 5 μm

Surgical procedures

All surgical procedures were performed by one experienced surgeon (Lanlei Wang). General anesthesia was performed with an intravenous injection of 3% pentobarbital sodium (Shanghai, China, 30 mg/kg). Labial mucoperiosteal flaps of the third incisor were raised on each side of the maxilla. The labial alveolar bone plate (5×3×5 mm) and the exposed periodontal ligament and cementum were removed. Reference notches indicating the bottom of the defect were made on the respective root surfaces with a high-speed handpiece under saline irrigation (Fig. 2a). All root surfaces in defects were conditioned with a 24% ethylenediaminetetraacetate (EDTA)-containing gel (MD-ChelCream™, Meta Biomed Co., Ltd, Korea) for 2 min. The surgical sites were rinsed thoroughly with sterile saline. The PBCP block was trimmed into granules of about 0.5–1 mm^3 and immersed into sterile saline. PBCP was randomly filled in one defect (Fig. 2b), and nothing was put in the contralateral as control. Finally, the flap was repositioned and sutured tightly with Gore-Tex CV-5 suture (W.L. Gore & Associates, Flagstaff, AZ, USA). Periodontal dressing (Drug Manufacturing Room, West China Stomatological Hospital of Sichuan University) was placed to protect the wound and removed 3 days later. The

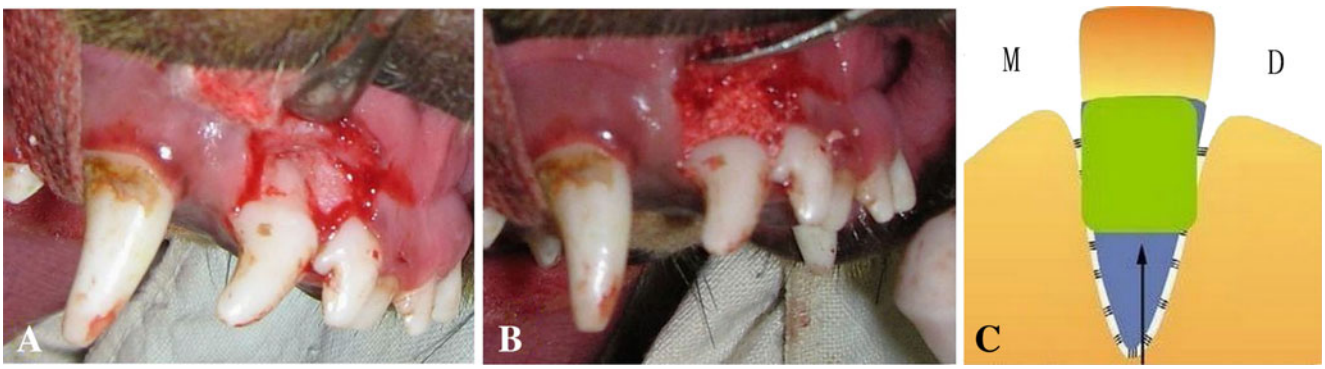

Fig. 2 **a** The alveolar bone block about 3 mm wide, 5 mm high and deep into the root surface was removed from the labial alveolar bone of the maxillary third incisor. The horizontal notch was made on the bottom of the root surface in the bone defect; **b** PBCP was filled in the right bone defect; **c** experimental periodontal defect model used in the present study. *green* bone defect, *M* mesial, *D* distal

animals received an antibiotic (penicillin G, 800,000 IU) administered intramuscularly once a day for three consecutive days. Sutures were removed 2 weeks later. Chemical plaque control (0.2% chlorhexidine rinsing and then iodine glycerin smearing) was performed once a day for 2 weeks and then reduced to twice a week (sterile saline rinsing and then iodine glycerin smearing) until the animals were sacrificed.

Sequential fluorescent labeling in vivo

Two fluorochrome labelings were administered: tetracycline (Amresco 0422, American), 20 mg/kg body weight, subcutaneous injection in the neck, 7 weeks postoperatively; xylenol orange (Sigma-Aldrich, Munich, Germany), 34 mg/kg body weight, subcutaneous injection in the neck, 11 weeks postoperatively.

Microcomputed tomography scan

Placed in a custom jig with foam filling void, the samples were immersed in 70% ethanol and were scanned by a micro-CT 80 scanner (μCT 80, Scanco Medical AG, Bassersdorf, Switzerland). Four hundred eighty projections were taken with a resolution of 1,024×1,024 pixels and with an isotropic voxel size of 18 μm.

Histological and histomorphometric analysis

Histological examinations

For hard tissue histology, the specimens were fixed in 70% ethanol for 3 days, dehydrated in ascending graded ethanol series, and then embedded in methylmethacrylate without decalcification. Five- and 10 μm histological sections were cut in the labiolingual direction, parallel to the long axes of the teeth with a microtome (Leica SM 2500E, Germany).

The sections of 5 μm were stained with hematoxylin and eosin and with toluidine blue before examination with a light microscope (Leica DMR). The images were captured by a digital camera connected to that light microscope. The sections of 10 μm were observed under a fluorescent microscope (LEICA DMI 6000B, The Netherlands) with an exposure of 5.5 s (DAPI-type and rhodamine-type filter sets for tetracycline and xylenol orange fluorescence, respectively), and photos were taken with an inbuilt image collection system.

Histomorphometric analysis of newly formed periodontal tissues

Histomorphometric analyses and microscopic observations were performed by Yijia Chen masked to the specific experimental conditions. For linear measurements, images were obtained at a magnification of ×100 by a digital camera connected to the light microscope (Leica DMR). Digital images were evaluated using a software program (SIS analysis Auto Software 3.2, Soft imaging System). The apical extension of the notch was used as the reference point. The height of new bone (NB), new cementum (NC), and new periodontal ligament (PDL) were, respectively, measured from the apical extension of the reference notch to the coronal extension of newly formed tissue along the root surface (Fig. 5). The comparison between test and control in terms of NB, NC, and PDL was performed using paired *t* test.

Experimental results

Clinical observations

All surgeries went well and the clinical incision healing was uneventful in all the animals. In all cases, no complications such as inflammation and exposure of PBCP were observed after implantation.

μCT examination

Qualitative analysis

The 3D images were obtained for qualitative and quantitative evaluation by an inbuilt global thresholding procedure (threshold 225 for teeth and host bone and threshold 170 for new alveolar bone). 3D reconstructed images and cross-section photos of the teeth were observed. The images revealed that much more new bone formed in PBCP groups (Fig. 3a, b) than that in the control group (Fig. 3c, d). The cross-section photos showed that newly formed alveolar bone was in perfect continuity with the host trabecular structure.

Quantitative analysis

Fifty continuous slices with new visible bone were selected from μCT images of each sample in PBCP group. The same volume of the new bones and the host bone near the notch were selected and measured for comparison by inbuilt software (Table 1). The following microarchitecture parameters were assessed: trabecular number, trabecular thickness, and trabecular separation, which provide detailed information on the amount, thickness, and organization of trabeculae. Maturity of new bones increased with time and each indicator got closer to the host bone.

Fluorescence analysis

Fluorescence labels were used to visualize newly formed bone. Sequential fluorochrome labels revealed the dynamics of bone formation. Fluorochrome, together with calcium,

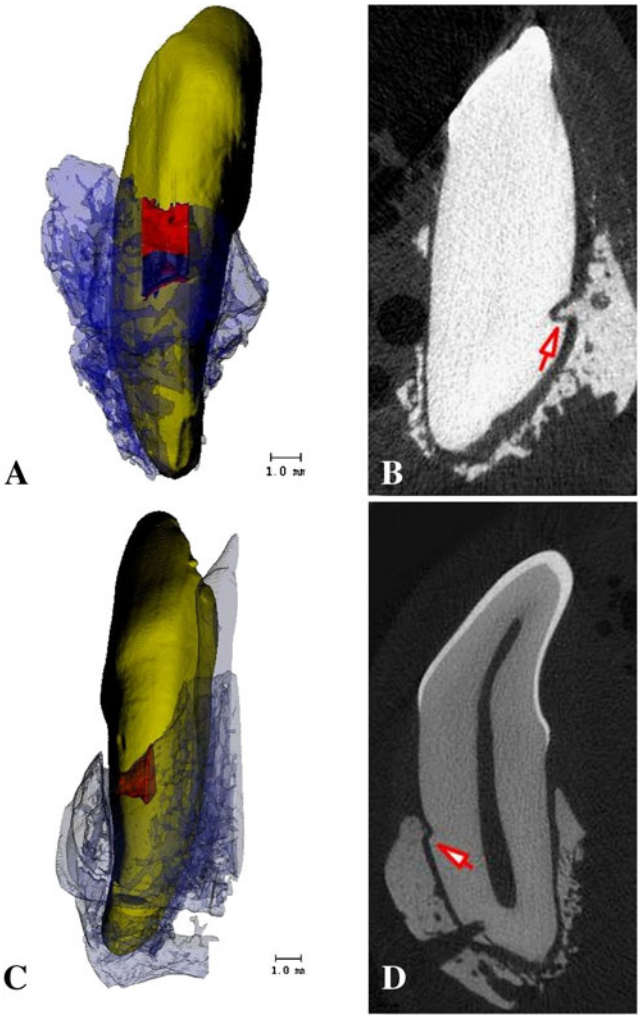

Fig. 3 Images of reconstructed sample and single slice, the specimens came from the same dog of 16 weeks. *Red* new bone, half transparent, *blue* host bone, *yellow* tooth. *Red arrows* point to the notch. **a** Reconstructed 3D images of specimen in PBCP group; there is abundant new bone. *Bar scales*, 1 mm; **b** the cross-section image of **a**; **c** reconstructed images of the tooth in the control group, new bone only cover the notch. *Bar scales*, 1 mm; **d** the cross-section image of **c**

was deposited in the bone formation process and stimulated by rays of specific wave length, the fluorochrome fluoresces, which indicates the locations of new bone depositing.

In this study, tetracycline and xylenol were administered at the 7th and 11th weeks, respectively. At 7 week postoperatively, tetracycline fluoresced yellow and a clear bright yellow fluorescent band showed up in PBCP group (Fig. 4a) while an obscure one in the control (Fig. 4b). At 11 week postoperatively, xylenol orange fluoresced orange and a fluorescent banding appeared in PBCP group (Fig. 4c) while obscure in the control group (Fig. 4d). It meant that there was much more active new bone mineralization in PBCP group than that in OFD group at the same time point.

In PBCP group (Fig. 4a, c), the yellow strip and the orange one were almost in the same position, which indicates that the quantity of the new bone was not increased and new bone mineralization had kept up between 7 and 11 weeks. From the photo of the controls (Fig. 4b, d), we may conclude that mineralization of new bone in the controls has been very weak at 7 and 11 weeks postoperatively.

Histological and histomorphometric analysis

Histomorphometric analysis of newly formed periodontal tissues

In PBCP groups, the amount of NB varied from 1.15 to 3.86 mm (23–77.2% of the original defect size which was 5 mm), while only 0.3 to 1.04 mm (6–20.8% of the original defect size) in OFD group. The amount of NC in PBCP varied from 1.18 to 4.16 mm (23.6–82.3% of the original defect size), while only 0.67 to 1.15 mm (13.4–23% of the original defect size) in OFD group. The amount of PDL in PBCP varied from 1.03 to 4.12 mm (20.6–82.4% of the original defect size), while only 0 to 0.93 mm (0–18.6% of the original defect size) in OFD group. Statistically significant differences were found between the two groups, which were in favor of the PBCP therapy ($p<0.01$; Fig. 5).

Table 1 Quantitative results about the newly formed bone of the experimental group

	Tb.N (1/mm)	Tb.Th (μm)	Tb.sp (mm)	BV (mm^3)	Mean density (mg HA/ccm)
12 weeks	0.9827	0.3745	0.4765	2.7657	658.7638±156.8765
16 weeks	1.2334	0.4928	0.3919	3.2713	714.7436±147.8743
24 weeks	1.7256	0.8976	0.2857	4.2123	826.5274±152.7646
HB	1.8120	1.0445	0.2219	4.3088	837.6048±153.8479

μCT scanning was processed at 12, 16, and 24 weeks

BV new bone volume, *Tb.N* trabecular number, *Tb.Th* trabecular thickness, *Tb.sp* trabecular separation, *HB* host alveolar bone (normal alveolar bone as control)

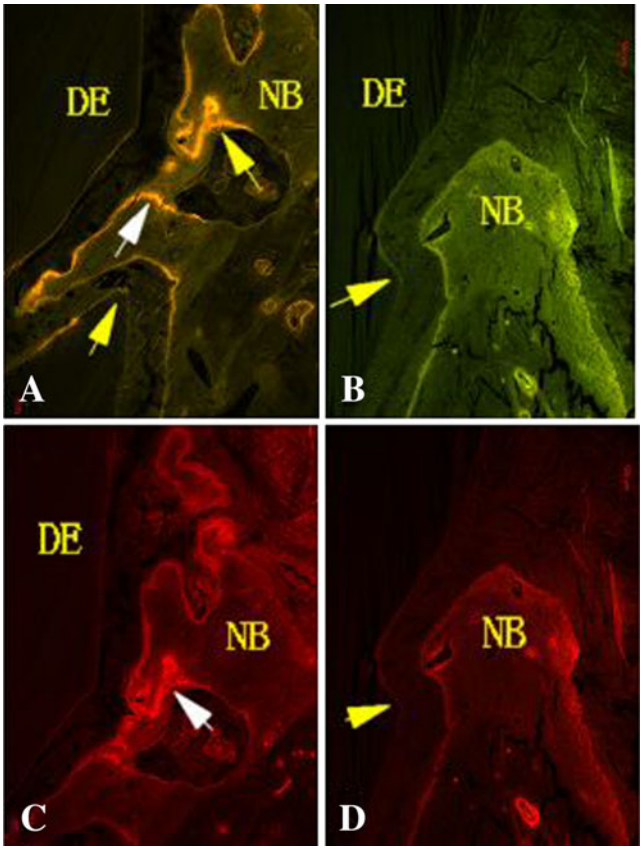

Fig. 4 Fluoresce images, *DE* dentin, *NB* new bone, *white arrow* pointed to the notch, *yellow arrow* pointed to the fluorochrome banding. All the *photographs* are taken from sections of the same dog. All **a** and **c** were obtained from the same section, so were Fig. **b** and **d**. **a** Tetracycline fluoresced yellow and a fluorochrome banding appeared in the new alveolar bone of PBCP group (×50); **b** fluorescence of tetracycline was obscure in the new bone of OFD group (×50); **c** xylenol orange fluoresced orange and a clear bright band showed up in the new bone of PBCP group (×50); **d** fluorescence of xylenol orange in the control group was obscure in the new bone of OFD group (×50)

Histological findings

Histological observation showed that the height of new bone was highly variable among the dogs. But in the same dog, PBCP have always demonstrated enhanced bone fill relative to OFD. So we randomly choose the photos of the same dog to compare bone fill of two groups (Fig. 6a, e). Most specimens exhibited a thick layer of new cementum in the notch area, whereas a thinner new cementum layer was observed more coronally. No signs of root resorption or ankylosis were observed in all the specimens. Artifacts (splits between the new cementum and the dentin surface) were often observed in specimens, irrespective of the treatment modality.

In PBCP groups, the new alveolar bone was integrated with host bone tightly without the formation of surrounding fibrous tissues, which showed PBCP had good bone-bonding ability. No identifiable PBCP residues were found in all specimens. Perpendicularly oriented collagen fibers inserted into the new cementum and connected to the newly formed bone (Fig. 6a–d). As time moved on, the new PDL was reorganized to functional alignment gradually in order to accommodate the masticatory function of the teeth: (1) at 12 weeks, new collagen fiber bundles mostly inclined to the crown with the end embedded in cementum higher than the other end buried in the new bone (Fig. 6b); (2) at 16 weeks, most fiber bundles had already aligned vertically to the root surface (Fig. 6c); and (3) at 24 weeks, new collagen fiber bundles were consistent with hosts ones at right angles (Fig. 6d, h). These findings seemed to prove that PBCP may have positive effects on periodontal wound healing and regeneration.

In OFD groups, no significant differences of newly formed PDL could be discerned between 12, 16, and 24 weeks either under low lens or under high lens. Limited periodontal regeneration formed at the most apical part of the defect. New mixed cementum without inserting collagen fibers deposited on the root surface in the notch. Thin and little, the newly formed fiber bundles were parallel to the root surface (Fig. 6f, g). It meant that the healing was still a periodontal repair instead of periodontal regeneration.

Discussion

PBCP has already been proven its efficacy on bone regeneration as a bone substitute in different clinical applications. When implanted in osseous sites, PBCP can form bone-like apatite on their surfaces in the living body, through which PBCP can bond directly to the living bone without an intervening fibrous layer. Contacting with the living bone, PBCP stimulate bone growth. The new cells

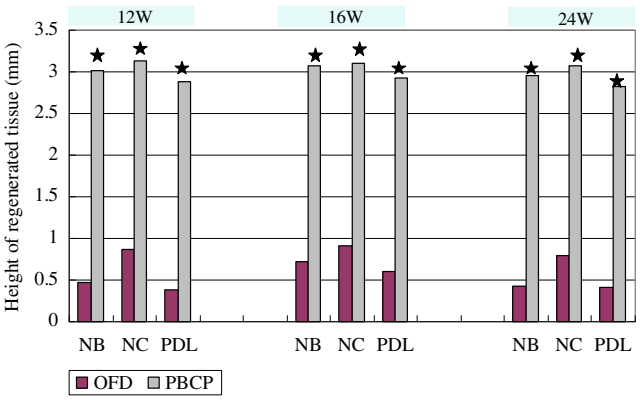

Fig. 5 Mean values (millimeters) of the linear measurements for regenerated periodontal tissues in both groups. *Star* significant against the values of OFD group ($p<0.01$)

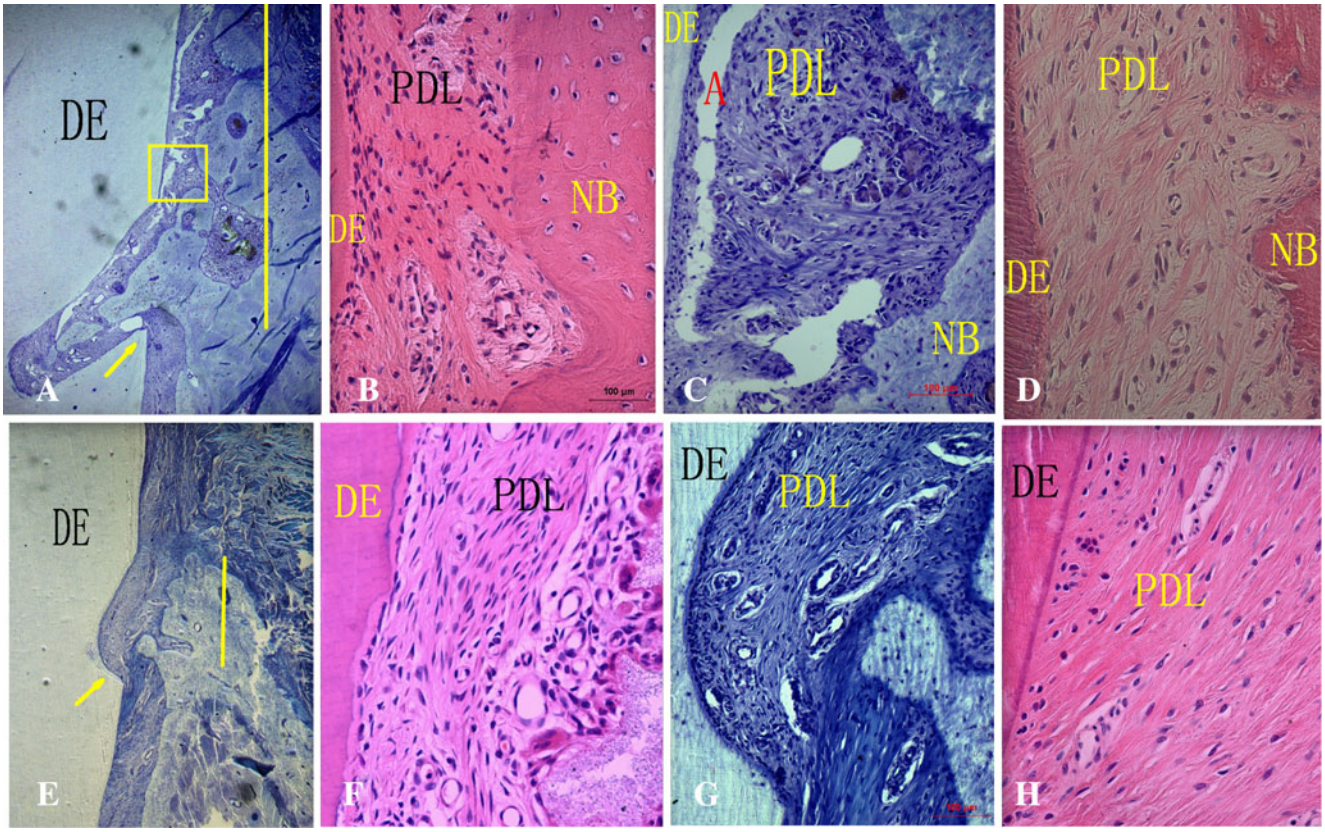

Fig. 6 Photomicrograph of healing. The sections of **a**, **c**, **e**, and **g** were stained with toluidine blue; the sections of **b**, **d**, **f**, and **h** were stained with hematoxylin and eosin (*yellow arrows* pointed to the notch, *yellow lines* marked the height of the new alveolar bone, *NB* new bone, *DE* dentin, *HB* host bone, *PDL* periodontal ligament); **a** 16 weeks in PBCP: healing resulted in abundant periodontal regeneration (×40); **b** 12 weeks in PBCP: new collagen fiber bundles mostly inclined to the crown with one end embedded in cementum higher than the other end buried in adjacent bone (×400); **c** 16 weeks in PBCP, magnified view of yellow rectangle in **a**: most fiber bundles aligned in vertical to the root surface (×200); **d** 24 weeks of PBCP: new collagen fiber bundles were in functional arrangement at right angles (×400); **e** 16 weeks in OFD: limited new alveolar bone formed in the defect and covered the notch at most (×40); **f** 12 weeks in OFD: new mixed cementum without inserting collagen fibers deposited on the root surface in the notch, the new PDL were thin and little, which parallel to the root surface (×400); **g** 16 weeks in OFD, magnified view of **e**, newly formed PDL were parallel to the root surface (×200); **h** magnified view of normal PDL just below the notch, collagen fiber bundles arranged orderly with one end embedded in cementum lower than the other end buried in adjacent bone at about 45° (×400)

grow within the material and progressively degrade it. The ceramic should be kept there until it is completely replaced by the new bone within a few weeks [13, 22, 23].

As for optimal bone regeneration, the degradation rate of PBCP should equalize the rate of bone ingrowths. The biodegradation of PBCP depends on many factors, such as HA/β-TCP ratio, porosity, degree of bony contact, specific surface, type of bone, species of animal, age, sex, etc. [24]. Ideally, when any factor varies, PBCP should be readjusted to accommodate the specific implantation site consequently. By adapting the proportions of HA/β-TCP and the pores structure, it is possible to control biodegradation of PBCP [10, 11]. However, it is still a challenge to optimize the appropriate porous structure and the composition of PBCP to accommodate bone-specific implantation sites.

An important factor affecting degradation of PBCP is the site of implant placement. The trabecular bone appears to allow more rapid tissue growth than the cortical bone presumably due to the richer vascularity of such structures [24]. In view of poor vascular supply of periodontal implant sites, PBCP in this study has a high porosity of 85% and possesses more biodegradable β-TCP than HA to facilitate its biodegradation. At 12, 16, and 24 weeks of healing, PBCP ceramics were absorbed completely and no residual material was found in the implant site.

An important factor affecting degradation of PBCP is its porous structure. Micropores and high porosity in PBCP result in larger surface area which can facilitate biodegradation. The characteristic feature of PBCP in this study was abundant micropores in the walls of interchanneled macropores, which promoted degradation greatly and accelerated interface bonding reaction.

In clinical application, scaffold materials should have an appropriate porous structure to mimic the complex archi-

tecture of bone-specific sites to optimize integration into the surrounding tissue. Trabecular bone creates a porous environment with 50–90% porosity, with cortical bone surrounding it. In trabecular bone, the pore diameters vary from 200 to 700 μm whereas in cortical bone, pore sizes range from 1 to 100 μm. The pore size, porosity, and interconnectivity of the pores are critical factors affecting tissue ingrowths, cell attachment, migration and expression, and diffusion of nutrients that are necessary for bone regeneration [13, 14, 25]. Thus, porosity, pore size, and pore geometry must be precisely balanced and controlled in order to optimize the overall performance of these bioceramics.

However, it is still not clear which is the optimal geometry and composition for bone substitutes although many studies have been looking for it. Optimal pore sizes have rarely been defined. It is generally admitted that macropores larger than 100–150 μm can facilitate ingrowth of mineralized bone [14]. Abundant microporosity is believed to contribute to higher bone inducing protein adsorption as well as to ion exchange and bone-like apatite formation by dissolution and reprecipitation [25].

In clinical practice, labial or buccal alveolar bone defects are commonly found in the teeth with periodontitis. In order to provide reference for clinical practice, acute alveolar bone dehiscence defects were designed in our previous study [21]. In view of repeatability, we adopted the same defect type in this study. The acute-type defects involved might not necessarily represent the real situation encountered in a chronic, plaque-infected periodontal defect. Isidor et al. have evidenced that regeneration of alveolar bone and cementum was comparable for both acute and chronic defect condition in monkeys [26]. One major risk of the acute defect model is spontaneous regeneration, so we designed the control defects to exclude healing by spontaneous regeneration. One significant drawback of this therapy method was the huge variability of the histometric healing outcomes. New bone ingrowths are affected by the degree of bony contact [24]. Though bony contact area in alveolar bone dehiscence defects was less than that in intrabony or fenestration defects, the volume of periodontal regeneration was obvious.

In this study, μCT reconstruction was adopted to visualize newly formed alveolar bone. The 2D images revealed significant gains in bone fill with PBCP compared to OFD procedures (Fig. 3b, d). From the 3D images, we can see visually much new bone formation in PBCP groups while minute in the controls (Fig. 3a, c). It seemed that PBCP and OFD groups had just differed in the quantities of newly formed bone.

However, the histological results revealed that in OFD groups the new collagen fibers were aligned parallel to the root surface and were not inserted into the new-formed cementum (Fig. 6f, g). So the healing of OFD groups was still characterized by a long junctional epithelium although limited new bone formed, which was in accordance with previous studies [21, 27, 28].

The histological results provided compelling evidence that PBCP resulted in periodontal regeneration characterized by the formation of a new attachment apparatus. The implant site became indistinguishable virtually from the host tissue in the images of μCT and histology, which showed that PBCP had bone-bonding ability. PBCP was biocompatible in this study as evidenced by the low amount of inflammatory cells and the absence of macroscopic signs of inflammation.

Conclusions

The present results indicate that PBCP may enhance periodontal regeneration in acute-type labial dehiscence defects. To achieve a more predictable regeneration, the addition of certain stimuli such as growth factors or stem cells incorporated into the PBCP may be of advantage. However, this has to be confirmed in future studies.

Conflicts of interest statement The research was sponsored by Ph. D. program foundation of Ministry of Education of China: 20060610085. The authors declare that they have no conflict of interest.

References

1. Caton JG, Greenstein GG (1993) Factors related to periodontal regeneration. Periodontol 2000 1:9–15
2. Brunsvold MA, Mellonig JT (1993) Bone grafts and periodontal regeneration. Periodontol 2000 1:80–91
3. Mellonig JT (1996) Bone allografts in periodontal therapy. Clin Orthop Relat R 324:116–125
4. Gestrelius S, Lyngstadaas SP, Hammarström L (2000) Emdogain—periodontal regeneration based on biomimicry. Clin Oral Invest 4:120–125
5. Sculean A, Donos N, Brecx M, Karring T, Reich E (2000) Healing of fenestration-type defects following treatment with guided tissue regeneration or enamel matrix proteins. An experimental study in monkeys. Clin Oral Invest 4:50–56
6. Sun WB, Chu CL, Wang J, Zhao HT (2007) Comparison of periodontal ligament cells responses to dense and nanophase hydroxyapatite. J Mater Sci Mater Med 18:677–683
7. Cetinkaya BO, Keles GC (2007) Comparison of the proliferative activity in gingival epithelium after surgical treatments of intrabony defects with bioactive glass and bioabsorbable membrane. Clin Oral Invest 11:61–68
8. Daculsi G (1998) Biphasic calcium phosphate concept applied to artificial bone, implant coating and injectable bone substitute. Biomaterials 19:1473–1478
9. Ellinger RF, Nery EB, Lynch KL (1986) Histological assessment of periodontal osseous defects following implantation of hydroxyapatite and biphasic calcium phosphate ceramics: a case report. J Period Res Dent 6(3):22–33

10. Will J, Melcher R, Treul C, Travitzky N (2008) Porous ceramic bone scaffolds for vascularized bone tissue regeneration. J Mater Sci Mater Med 19:2781–2790
11. Heymann D, Passuti N (1999) Bone substitutes: new concepts. Eur J Orthop Surg Traumatol 9:179–184
12. Gauthier O, Boulerb JM, Aguado E, Piletb P, Daculsib G (1998) Macroporous biphasic calcium phosphate ceramics: influence of macropore diameter and macroporosity percentage on bone ingrowth. Biomaterials 19:133–139
13. LeGeros RZ (2002) Properties of osteoconductive biomaterials: calcium phosphates. Clin Ortho Relat R 395:81–98
14. Yuan HP, Yang ZJ, Li YB, Zhang XD, De Bruijn JD, De Groot K (1998) Osteoinduction by calcium phosphate biomaterials. J Mater Sci Mater Med 9(12):723–726
15. Klein C, Degroot K, Chen WQ, Li YB, Zhang XD (1994) Osseous substance formation induced in porous calcium-phosphate ceramics in soft-tissues. Biomaterials 15(1):31–34
16. Nihouannen DL, Saffarzadeh A, Gauthier O (2008) Bone tissue formation in sheep muscles induced by a biphasic calcium phosphate ceramic and fibrin glue composite. J Mater Sci Mater Med 19:667–675
17. Nihouannen DL, Daculsi G, Saffarzadeh A, Gauthier O, Delplace S, Pilet P, Layrolle P (2005) Ectopic bone formation by microporous calcium phosphate ceramic particles in sheep muscles. Bone 36:1086–1093
18. Yuan HP, Yang ZJ, Yuan LI (1998) Osteoinduction by calcium phosphate biomaterials. J Mater Sci Mater Med 9:723–726
19. Zhu XD, Fan HS, Xiao YM, Li DX, Zhang HJ, Luxbacher T (2009) Effect of surface structure on protein adsorption to biphasic calcium-phosphate ceramics in vitro and in vivo. Acta Biomater 5:1311–1318
20. Sun L, Wu L, Bao C, Fu C, Wang X, Yao J, Zhang X, Blitterswijk CAV (2009) Gene expressions of collagen type I, ALP and BMP-4 in osteo-inductive BCP implants show similar pattern to that of natural healing bones. Mat Sci Eng C 29:1829–1834
21. Shi H, Ma J, Zhao N, Chen YX, Liao YM (2008) Periodontal regeneration in experimentally-induced alveolar bone dehiscence by an improved porous biphasic calcium phosphate ceramic in beagle dogs. J Mater Sci Mater Med 19:3515–3524
22. Ducheyne P, Qiu Q (1999) Bioactive ceramics: the effect of surface reactivity on bone formation and bone cell function. Biomaterials 20:2287–2303
23. Kokubo T, Matsushita T, Takadama H, Kizuki T (2009) Development of bioactive materials based on surface chemistry. J Eur Ceram Soc 29:1267–1274
24. Passuti N, Delécrin J, Daculsi G (1997) Experimental data regarding macroporous biphasic calcium phosphate ceramics. Eur J Orthop Surg Traumatol 7:79–84
25. Karageorgiou V, Kaplan D (2005) Porosity of 3D biomaterial scaffolds and osteogenesis. Biomaterials 26:5474–5491
26. Isidor F, Karring T, Nyman S, Lindhe J (1985) New attachment–reattachment following reconstructive periodontal surgery. J Clin Periodontol 12:728–735
27. Schwarz F, Stratul S, Herten M, Beck B, Becker J, Sculean A (2006) Effect of an oily calcium hydroxide suspension (Osteoinductal) on healing of intrabony periodontal defects. A pilot study in dogs. Clin Oral Invest 10:29–34
28. Beck B, Becker J, Sculean A (2006) Effect of an oily calcium hydroxide suspension (Osteoinductal) on healing of intrabony periodontal defects. A pilot study in dogs. Clin Oral Invest 10:29–34

Copyright of Clinical Oral Investigations is the property of Springer Science & Business Media B.V. and its content may not be copied or emailed to multiple sites or posted to a listserv without the copyright holder's express written permission. However, users may print, download, or email articles for individual use.